PHILOSOPHICAL MAGAZINE, 21 August 2004
VOL. 84, NO. 24, 2543–2557

Taylor & Francis
Taylor & Francis Group

Ab initio determination of the optical properties of bulk Au and free surfaces of Au

I. REICHL†, A. VERNES†, L. SZUNYOGH†‡, C. SOMMERS §,
P. MOHN† and P. WEINBERGER†

† Center for Computational Materials Science, Technical University of Vienna, Getreidemarkt 9/134, A-1060 Vienna, Austria
‡ Department of Theoretical Physics, Institute of Physics, Budapest University of Technology and Economics, Budafoki út 8, H-1521 Budapest, Hungary
§ Laboratoire de Physique des Solides, Université de Paris-Sud, 91405 Orsay Cedex, France

[*Received 5 March 2004 and accepted 5 March 2004*]

ABSTRACT

The optical properties of bulk Au and a (100) free surface of Au are determined by solving the Helmholtz–Fresnel equations for a geometry reflecting layered systems. This approach is based on the use of the microscopical conductivity tensor evaluated fully relativistically and, for later purposes, does include the option of choosing an arbitrary uniform direction of a possibly present magnetization. It will be shown that, while so-called experimental bulk data agree reasonably well with their theoretically obtained counterparts, in the case of free surfaces of Au (semi-infinite systems) they not only disagree substantially in size between different experiments but also with the theoretical values. The shapes of the curves for the real and the imaginary parts of the diagonal permittivity tensor elements ε_{xx} and ε_{zz}, however, are rather similar.

§ 1. INTRODUCTION

There is no question that optical measurements, and in particular magneto-optical investigations based on the Kerr effect are of great importance not only in academic research but also on the industrial level (see for example the review article by Weller (1995)). A theoretical description of such experiments and techniques, however, has to deal with two important aspects, namely with a description of the actual optical phenomenon, which of course belongs to classical physics (Mansuripur 2002) and the underlying microscopic origin in terms of a quantum-mechanically defined optical conductivity tensor. This distinction between macroscopic and microscopic quantities becomes especially important in dealing with multilayer systems such as magnetically coated metals serving as a suitable substrate. Furthermore, since any kind of optical measurement has to be carried out from the 'outside' of the system to be investigated, that is it refers to a realistic system with a defined surface, a surface near region and a buried interior, theoretical means have to reflect properly the condition of being adequately realistic.

† Author for correspondence. Email: pw@cms.tuwien.ac.at.

Philosophical Magazine ISSN 1478–6435 print/ISSN 1478–6443 online
http://www.tandf.co.uk/journals
DOI: 10.1080/14786430410001693445

In the present paper the main emphasis is put on the optical part of determining permittivities. For this reason a system is chosen which very often serves as a substrate for various kinds of magnetic multilayer system, namely pure Au. Although this appears to be an easy example it will be shown that any sort of comparison with experimental data has to be made with great care; depending on the methods applied to produce experimentally suitable samples, substantial differences in the optical properties can be found in the literature. In the following a method is described to deal with all reflections and interferences of a system caused by incident light parallel to the surface normal, but keeping the orientation of a possibly present magnetization general, that is not restricting the magnetization to point along the surface normal.

§ 2. Optical properties of a layered system

The optical properties of a material can be described by the well-known Helmholtz equation

$$n^2\boldsymbol{E} - \boldsymbol{\varepsilon}\boldsymbol{E} - (\boldsymbol{n}\cdot\boldsymbol{E})\boldsymbol{n} = \boldsymbol{0},$$

where $\boldsymbol{\varepsilon}$ is the permittivity tensor, $\boldsymbol{n}$ the refraction vector and $\boldsymbol{E}$ the electric field. Since in thin-film systems the permittivity varies with the distance to the surface, this equation has to be reformulated such that it can be expressed in layer-resolved quantities. In the following, first the solutions of the Fresnel equation are discussed in a single layer and then boundary conditions will be introduced in order to join up the layer-resolved quantities.

2.1. *The solution of the Helmholtz equation in one layer*

Consider a solid magnetized homogeneously in an arbitrary direction, and let the incident light be parallel to the surface normal (z axis, normal to the x–y plane). The layer-resolved permittivity tensor $\boldsymbol{\varepsilon}^p$ and refraction vector $\boldsymbol{n}_p$ are then of the form

$$\boldsymbol{\varepsilon}^p = \begin{pmatrix} \varepsilon^p_{xx} & \varepsilon^p_{xy} & \varepsilon^p_{xz} \\ \varepsilon^p_{yx} & \varepsilon^p_{yy} & \varepsilon^p_{yz} \\ \varepsilon^p_{zx} & \varepsilon^p_{zy} & \varepsilon^p_{zz} \end{pmatrix}, \quad \boldsymbol{n}_p = \begin{pmatrix} 0 \\ 0 \\ n_p \end{pmatrix}.$$

It should be noted that, in contrast with the work of Vernes *et al.* (2002a, b), in this paper this form of $\boldsymbol{\varepsilon}^p$ corresponds to a general orientation of the magnetization of the surface.

In order to determine $\boldsymbol{n}_p$ the Fresnel equation

$$\det\left(\boldsymbol{n}_p^2\delta_{\mu\nu} - \varepsilon^p_{\mu\nu} - n_{p,\mu}n_{p,\nu}\right) = 0, \quad \mu,\nu \in \{x,y,z\},$$

has to be solved. Since in this equation only even powers of n_p occur, the corresponding solutions $\{n_p^{(k)}\}, k = 1,\ldots,4$, have the property that

$$n_p^{(1)} = -n_p^{(3)}, \quad n_p^{(2)} = -n_p^{(4)},$$

which in turn implies that these four solutions yield only two different systems of equations and therefore only two linear independent solutions can be obtained for the time-independent part of the electric field vector $\boldsymbol{E}_p^{(k)}$.

The components of each wave can be expressed in terms of one component, for example

$$\boldsymbol{E}_p^{(k)} = \begin{pmatrix} E_{p,x}^{(k)} \\ E_{p,y}^{(k)}(E_{p,x}^{(k)}) \\ E_{p,z}^{(k)}(E_{p,x}^{(k)}) \end{pmatrix}, \quad k = 1, 3.$$

Describing multiple reflections of light at normal incidence, it is therefore sufficient to take only the x and the y components into account. The monochromatic, homogeneous and harmonic plane waves are then given by

$$\boldsymbol{E}_p^{(k)}(z, t) = \boldsymbol{E}_p^{(k)} \exp\left[\mathrm{i}(\tilde{q}_p z - \tilde{\omega} t)\right], \quad \tilde{q}_p = q_0 n_p^{(k)}, \quad \tilde{\omega} = \omega - \mathrm{i}\delta, \tag{1}$$

where q_0, given by

$$q_0 = \frac{\omega}{c},$$

is the propagation constant in vacuum, ω is the photon frequency and δ is the lifetime broadening parameter (Szunyogh and Weinberger 1999, Vernes *et al*. 2002a, c). For later purposes it is necessary to identify the incident and the reflected waves at each interface. It is convenient to define waves with $n_p^{(1)}$ and $n_p^{(2)}$ $(\mathrm{Im}\,(n_p^{(k)}) < 0,\ k = 1, 2)$ as incident waves and waves with $n_p^{(3)}$ and $n_p^{(4)}(\mathrm{Im}\,(n_p^{(k)}) > 0,\ k = 3, 4)$ as reflected waves.

The total incident wave (indicated by the superscript inc) is a linear combination of $\boldsymbol{E}_p^{(1)}$ and $\boldsymbol{E}_p^{(2)}$, which by introducing a 2×2 matrix can be written as a function of the x component of $\boldsymbol{E}_p^{(1)}$ and the y component of $\boldsymbol{E}_p^{(2)}$:

$$\begin{pmatrix} E_{p,x}^{\mathrm{inc}} \\ E_{p,y}^{\mathrm{inc}} \end{pmatrix} = \mathbf{A}_p \begin{pmatrix} E_{p,x}^{(1)} \\ E_{p,y}^{(2)} \end{pmatrix}, \tag{2}$$

where

$$\mathbf{A}_p = \begin{pmatrix} 1 & \dfrac{E_{p,x}^{(2)}(E_{p,y}^{(2)})}{E_{p,y}^{(2)}} \\ \dfrac{E_{p,y}^{(1)}(E_{p,x}^{(1)})}{E_{p,x}^{(1)}} & 1 \end{pmatrix}.$$

It is easy to find the matrix $\mathbf{A}_p'$ which connects the reflected wave to $\boldsymbol{E}_p^{(3)}$ and $\boldsymbol{E}_p^{(4)}$. The waves $\boldsymbol{E}_p^{(k)}$ and $\boldsymbol{E}_p^{(k+2)}, k = 1, 2$, differ only by a phase factor such that

$$\frac{E_{p,x}^{(3)}}{E_{p,y}^{(3)}} = \frac{E_{p,x}^{(1)}}{E_{p,y}^{(1)}}, \qquad \frac{E_{p,x}^{(4)}}{E_{p,y}^{(4)}} = \frac{E_{p,x}^{(2)}}{E_{p,y}^{(2)}},$$

which in turn implies that $\mathbf{A}_p' \equiv \mathbf{A}_p$.

Defining now a general 2×2 reflection matrix $\mathbf{R}_p$ which transforms the x and y components of the incident waves, $\boldsymbol{E}^{(1)}$ and $\boldsymbol{E}^{(2)}$, into their reflected counterparts (indicated by the superscript ref), $\boldsymbol{E}^{(3)}$ and $\boldsymbol{E}^{(4)}$, the total reflected wave is given by

$$\begin{pmatrix} E_{p,x}^{\mathrm{ref}} \\ E_{p,y}^{\mathrm{ref}} \end{pmatrix} = \mathbf{A}_p \mathbf{R}_p \begin{pmatrix} E_{p,x}^{(1)} \\ E_{p,y}^{(2)} \end{pmatrix}. \tag{3}$$

As for each solution $\boldsymbol{n}_p^{(k)}$ (the superscript (k) numbers the solutions) the magnetic field vector $\boldsymbol{H}_p^{(k)}$ is given by

$$\boldsymbol{H}_p^{(k)} = \boldsymbol{n}_p^{(k)} \times \boldsymbol{E}_p^{(k)}, \quad k = 1, \ldots, 4,$$

and the above 2×2 matrix formalism yields

$$\begin{pmatrix} H_{p,x}^{\text{inc}} \\ H_{p,y}^{\text{inc}} \end{pmatrix} = \mathbf{N}_p \begin{pmatrix} E_{p,x}^{(1)} \\ E_{p,y}^{(2)} \end{pmatrix}, \tag{4}$$

$$\begin{pmatrix} H_{p,x}^{\text{ref}} \\ H_{p,y}^{\text{ref}} \end{pmatrix} = -\mathbf{N}_p \mathbf{R}_p \begin{pmatrix} E_{p,x}^{(1)} \\ E_{p,y}^{(2)} \end{pmatrix}, \tag{5}$$

where $\mathbf{N}_p$ is given by

$$\mathbf{N}_p = \begin{pmatrix} \dfrac{-n_p^{(1)} E_{p,y}^{(1)}(E_{p,x}^{(1)})}{E_{p,x}^{(1)}} & -n_p^{(2)} \\ n_p^{(1)} & \dfrac{n_p^{(2)} E_{p,x}^{(2)}(E_{p,y}^{(2)})}{E_{p,y}^{(2)}} \end{pmatrix}. \tag{6}$$

2.2. *Boundary conditions*

Between different layers the electric and the magnetic fields have to be matched at each boundary z_p (figure 1). The wave with the subscript z_p^+ is supposed to be the solution in the pth layer at the lower boundary z_p^+; the wave with the subscript z_p^- is the solution in the $(p-1)$th layer at the upper boundary z_p^-. At z_p^+ the sum of the

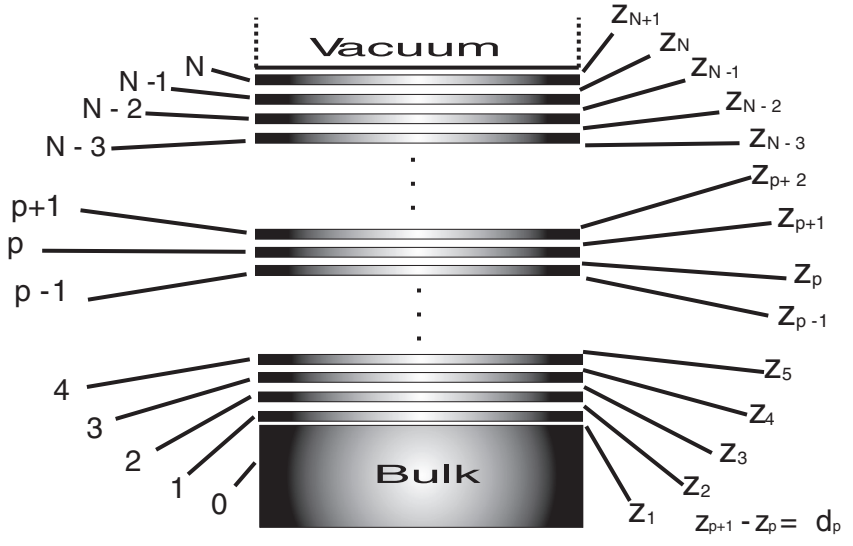

Figure 1. Layers are numbered from 1 to N; for the bulk regime the index 0 applies. Each layer p has a lower boundary z_p and an upper boundary z_{p+1}.

incident and the reflected wave applies (see equations (2)–(5)):

$$(\boldsymbol{E}_p)_{z_p^+} \equiv \begin{pmatrix} E_{p,x} \\ E_{p,y} \end{pmatrix}_{z_p^+} = \mathbf{A}_p(\mathbf{1} + \mathbf{R}_p)\begin{pmatrix} E_{p,x}^{(1)} \\ E_{p,y}^{(2)} \end{pmatrix}, \tag{7}$$

$$(\boldsymbol{H}_p)_{z_p^+} \equiv \begin{pmatrix} H_{p,x} \\ H_{p,y} \end{pmatrix}_{z_p^+} = \mathbf{N}_p(\mathbf{1} - \mathbf{R}_p)\begin{pmatrix} E_{p,x}^{(1)} \\ E_{p,y}^{(2)} \end{pmatrix}, \tag{8}$$

where $\mathbf{1}$ is the 2×2 unit matrix.

Because of the finite thickness d_{p-1} of layer $p-1$ the total wave at the lower boundary z_p^- is augmented by a phase shift $\varphi_{p-1}^{(k)}$ with respect to z_{p-1}^+:

$$\varphi_{p-1}^{(k)} = n_{p-1}^{(k)} q_0 d_{p-1}.$$

For $k=1$ or $k=3$ the matrix $\mathbf{C}_{p-1}^{(k,k+1)}$ given by

$$\mathbf{C}_{p-1}^{(k,k+1)} = \begin{pmatrix} \exp\left(\mathrm{i}\varphi_{p-1}^{(k)}\right) & 0 \\ 0 & \exp\left(\mathrm{i}\varphi_{p-1}^{(k+1)}\right) \end{pmatrix} \tag{9}$$

describes the wave propagation in layer $p-1$ from z_{p-1}^+ to z_p^-:

$$(\boldsymbol{E}_p)_{z_p^-} \equiv \begin{pmatrix} E_{p,x} \\ E_{p,y} \end{pmatrix}_{z_p^-} = \mathbf{A}_{p-1}\left(\mathbf{C}_{p-1}^{(1,2)} + \mathbf{C}_{p-1}^{(3,4)}\mathbf{R}_{p-1}\right)\begin{pmatrix} E_{p-1,x}^{(1)} \\ E_{p-1,y}^{(2)} \end{pmatrix}, \tag{10}$$

$$(\boldsymbol{H}_p)_{z_p^-} \equiv \begin{pmatrix} H_{p,x} \\ H_{p,y} \end{pmatrix}_{z_p^-} = \mathbf{N}_{p-1}\left(\mathbf{C}_{p-1}^{(1,2)} - \mathbf{C}_{p-1}^{(3,4)}\mathbf{R}_{p-1}\right)\begin{pmatrix} E_{p-1,x}^{(1)} \\ E_{p-1,y}^{(2)} \end{pmatrix}. \tag{11}$$

The boundary conditions, namely the continuity of the tangential components at z_p,

$$(\boldsymbol{E}_p)_{z_p^+} = (\boldsymbol{E}_{p-1})_{z_p^-},$$
$$(\boldsymbol{H}_p)_{z_p^+} = (\boldsymbol{H}_{p-1})_{z_p^-},$$

lead then to a set of equations for $(E_{p,x}^{(1)}, E_{p,y}^{(2)})$ and $(E_{p-1,x}^{(1)}, E_{p-1,y}^{(2)})$. After elimination of these pseudovectors an explicit expression for $\mathbf{R}_p$ is obtained:

$$\mathbf{R}_p = \left[\mathbf{N}_p + \mathbf{D}_{p-1}\mathbf{A}_p\right]^{-1}\left[\mathbf{N}_p - \mathbf{D}_{p-1}\mathbf{A}_p\right], \tag{12}$$

where $\mathbf{D}_{p-1}$ is defined by

$$\mathbf{D}_{p-1} = \mathbf{N}_{p-1}\left(\mathbf{C}_{p-1}^{(1,2)} - \mathbf{C}_{p-1}^{(3,4)}\mathbf{R}_{p-1}\right)\left(\mathbf{C}_{p-1}^{(1,2)} + \mathbf{C}_{p-1}^{(3,4)}\mathbf{R}_{p-1}\right)^{-1}\mathbf{A}_{p-1}^{-1}. \tag{13}$$

Equations (12) and (13) have to be solved recursively starting with $p=1$, namely the boundary between the substrate and the first layer. For $p = N+1$ the corresponding reflectivity matrix $\mathbf{R}_{\mathrm{surf}}$ is the surface reflectivity matrix.

2.3. *Recursive algorithm*

2.3.1. *Initial step*

Applying equations (12) and (13) for the boundary between the substrate and first layer, $\mathbf{N}_0$ can be determined using the refractive indices of the bulk system. Since in an ideal bulk system there are no boundaries and therefore no reflections,

the corresponding reflectivity matrix $\mathbf{R}_0$ can be assumed to be zero and thus

$$\mathbf{D}_0 = \mathbf{N}_0\mathbf{A}_0^{-1}, \tag{14}$$

$$\mathbf{R}_1 = (\mathbf{N}_0\mathbf{A}_0^{-1}\mathbf{A}_1 + \mathbf{N}_1)^{-1}(\mathbf{N}_1 - \mathbf{N}_0\mathbf{A}_0^{-1}\mathbf{A}_1). \tag{15}$$

2.3.2. *Last step*

Taking into account that there are only two solutions in the vacuum, namely one incident and one reflected wave, the reflectivity matrix at the vacuum interface (usually termed the surface reflectivity matrix) is given by

$$\mathbf{R}_{\text{surf}} = \begin{pmatrix} r_{xx} & r_{xy} \\ r_{yx} & r_{yy} \end{pmatrix}.$$

Furthermore, the material properties in vacuum are obtained when setting $n_p^{(1)}$ and $n_p^{(2)}$ to unity, that is

$$\mathbf{N}_{\text{vac}} = \begin{pmatrix} 0 & 1 \\ -1 & 0 \end{pmatrix}.$$

At z_{N+1}^{+} the total fields are therefore given by

$$[\boldsymbol{E}_{\text{vac}}]_{z_{N+1}^{+}} = (\mathbf{1} + \mathbf{R}_{\text{surf}})\boldsymbol{E}_{\text{vac}}^{(\text{inc})},$$

$$[\boldsymbol{H}_{\text{vac}}]_{z_{N+1}^{+}} = \mathbf{N}_{\text{vac}}(\mathbf{1} - \mathbf{R}_{\text{surf}})\boldsymbol{H}_{\text{vac}}^{(\text{inc})},$$

while at z_{N+1}^{-} they are of the form ($p = N$)

$$\begin{pmatrix} E_{\text{vac},x} \\ E_{\text{vac},y} \end{pmatrix}_{z_{N+1}^{-}} = \mathbf{A}_N\left(\mathbf{C}_N^{12} + \mathbf{C}_N^{34}R_N\right)\begin{pmatrix} E_{N,x}^{(1)} \\ E_{N,y}^{(2)} \end{pmatrix},$$

$$\begin{pmatrix} H_{\text{vac},x} \\ H_{\text{vac},y} \end{pmatrix}_{z_{N+1}^{-}} = \mathbf{N}_N\left(\mathbf{C}_N^{12} - \mathbf{C}_N^{34}\mathbf{R}_N\right)\begin{pmatrix} E_{N,x}^{(1)} \\ E_{N,y}^{(2)} \end{pmatrix}.$$

Demanding continuity at the surface for both fields leads to

$$\mathbf{R}_{\text{surf}} = (\mathbf{N}_{\text{vac}} + \mathbf{D}_N)^{-1}(\mathbf{N}_{\text{vac}} - \mathbf{D}_N), \tag{16}$$

$$\mathbf{D}_N = \mathbf{N}_N\left(\mathbf{C}_N^{(1,2)} - \mathbf{C}_N^{(3,4)}\mathbf{R}_N\right)\left(\mathbf{C}_N^{(1,2)} + \mathbf{C}_N^{(3,4)}\mathbf{R}_N\right)^{-1}\mathbf{A}_N^{-1}. \tag{17}$$

Equations (16) and (17) are the corresponding equations for the vacuum-surface interface which are needed to determine $\mathbf{R}_{\text{surf}}$.

§ 3. *Ab initio* determination of the permittivity tensor

3.1. *Recursive determination of* $\boldsymbol{\varepsilon}^p$

It was shown by Vernes *et al.* (2002a) that the (macroscopic) permittivity tensor $\boldsymbol{\varepsilon}^{pq}$ can be related to the (microscopic) conductivity tensor $\boldsymbol{\sigma}^{pq}$ in terms of the following mapping:

$$\varepsilon_{ij}^{pq}(\omega) = \delta_{ij}^{pq} + \frac{4\pi i}{\widetilde{\omega}}\sigma_{ij}^{pq}(\omega), \quad p, q = 1, \ldots, N, \quad \delta_{ij}^{pq} = \delta_{ij}\delta_{pq},$$

where N is the total number of (atomic) layers and $i, j \in \{x, y, z\}$. In order to obtain a layer-resolved reduced permittivity $\boldsymbol{\varepsilon}^p$, the implicit equation

$$\boldsymbol{\varepsilon}^p(\omega)\boldsymbol{E}_p = \sum_{q=1}^{N} \boldsymbol{\varepsilon}^{pq}(\omega)\boldsymbol{E}_q, \quad p = 1, \ldots, N, \tag{18}$$

has to be solved such that, when for example $\varepsilon^p_{yy} = \varepsilon^p_{xx}$ and $\varepsilon^p_{yx} = -\varepsilon^p_{xy}$,

$$\begin{pmatrix} \varepsilon^p_{xx} & \varepsilon^p_{xy} \\ \varepsilon^p_{yx} & \varepsilon^p_{yy} \end{pmatrix} \begin{pmatrix} E_{p,x} \\ E_{p,y} \end{pmatrix} = \sum_{q=1}^{N} \begin{pmatrix} \varepsilon^{pq}_{xx} & \varepsilon^{pq}_{xy} \\ \varepsilon^{pq}_{yx} & \varepsilon^{pq}_{yy} \end{pmatrix} \begin{pmatrix} E_{q,x} \\ E_{q,y} \end{pmatrix}, \quad p = 1, \ldots, N. \tag{19}$$

Shifting the index p in equation (10) to $p+1$,

$$\begin{pmatrix} E_{p+1,x} \\ E_{p+1,y} \end{pmatrix}_{z^-_{p+1}} = \mathbf{A}_p \left(\mathbf{C}^{(1,2)}_p + \mathbf{C}^{(3,4)}_p \mathbf{R}_p \right) \begin{pmatrix} E^{(1)}_{p,x} \\ E^{(2)}_{p,y} \end{pmatrix}, \tag{20}$$

the pseudovector $(E^{(1)}_{p,x}, E^{(2)}_{p,y})$ can be expressed in terms of equation (20) and inserted into equation (7) to yield

$$\begin{pmatrix} E_{p,x} \\ E_{p,y} \end{pmatrix}_{z^+_p} = \mathbf{A}_p (\mathbf{1} + \mathbf{R}_p) \left(\mathbf{C}^{(1,2)}_p + \mathbf{C}^{(3,4)}_p \mathbf{R}_p \right)^{-1} \mathbf{A}_p^{-1} \begin{pmatrix} E_{p+1,x} \\ E_{p+1,y} \end{pmatrix}_{z^-_{p+1}}. \tag{21}$$

$(\boldsymbol{E}_p)_{z^+_p}$ describes a wave at the boundary between layer $p-1$ and layer p. At half-distance between z_p and z_{p+1} this wave accumulates a phase shift which can be taken into account using a factor $(\mathbf{C}^{(k,k+1)}_p)^{1/2}$, $k = 1, 3$, such that each partial wave is multiplied automatically by the correct phase factor,

$$\begin{pmatrix} E_{p,x} \\ E_{p,y} \end{pmatrix}_{z^+_p + d_p/2} = \mathbf{A}_p \left[\left(\mathbf{C}^{(1,2)}_p \right)^{1/2} + \left(\mathbf{C}^{(3,4)}_p \right)^{1/2} \mathbf{R}_p \right] \begin{pmatrix} E^{(1)}_{p,x} \\ E^{(2)}_{p,y} \end{pmatrix}. \tag{22}$$

By replacing $(E^{(1)}_{p,x}, E^{(2)}_{p,y})$ in equation (22) with equation (20) and recursively inserting equation (21) into equation (22) $(\boldsymbol{E}_p)_{z^+_p + d_p/2}$ can finally be written as a function of $(\boldsymbol{E}_N)_{z^-_N}$:

$$\begin{pmatrix} E_{p,x} \\ E_{p,y} \end{pmatrix}_{z^+_p + d_p/2} = \prod_{k=p}^{N} \overline{\mathbf{W}}_k \begin{pmatrix} E_{N,x} \\ E_{N,y} \end{pmatrix}_{z^-_N} = \prod_{k=0}^{N-p} \overline{\mathbf{W}}_{k+p} \begin{pmatrix} E_{N,x} \\ E_{N,y} \end{pmatrix}_{z^-_N}, \tag{23}$$

where the matrices $\overline{\mathbf{W}}_{k+p}$ are defined in the following way:

$$\overline{\mathbf{W}}_{p+k} = \mathbf{A}_p \left[\left(\mathbf{C}^{(1,2)}_p \right)^{1/2} + \left(\mathbf{C}^{(3,4)}_p \right)^{1/2} \mathbf{R}_p \right] \left[\mathbf{C}^{(1,2)}_p + \mathbf{C}^{(3,4)}_p \mathbf{R}_p \right]^{-1} \mathbf{A}_p^{-1}, \quad k = 0,$$

$$\overline{\mathbf{W}}_{p+k} = \mathbf{A}_{p+k} (\mathbf{1} + \mathbf{R}_{p+k}) \left(\mathbf{C}^{(1,2)}_{p+k} + \mathbf{C}^{(3,4)}_{p+k} \mathbf{R}_{p+k} \right)^{-1} \mathbf{A}^{-1}_{p+k}, \quad k > 0.$$

The reduced permittivity $\boldsymbol{\varepsilon}^p$ is obtained by inserting the expansion in equation (23) into equation (18):

$$\boldsymbol{\varepsilon}^p(\omega) = \sum_{q=1}^{N} \boldsymbol{\varepsilon}^{pq}(\omega) \mathbf{W}_{pq},$$

$$\mathbf{W}_{pq} = \left(\prod_{k=0}^{N-q} \overline{\mathbf{W}}_{k+q} \right) \left(\prod_{k=0}^{N-p} \overline{\mathbf{W}}_{k+p} \right)^{-1}. \tag{24}$$

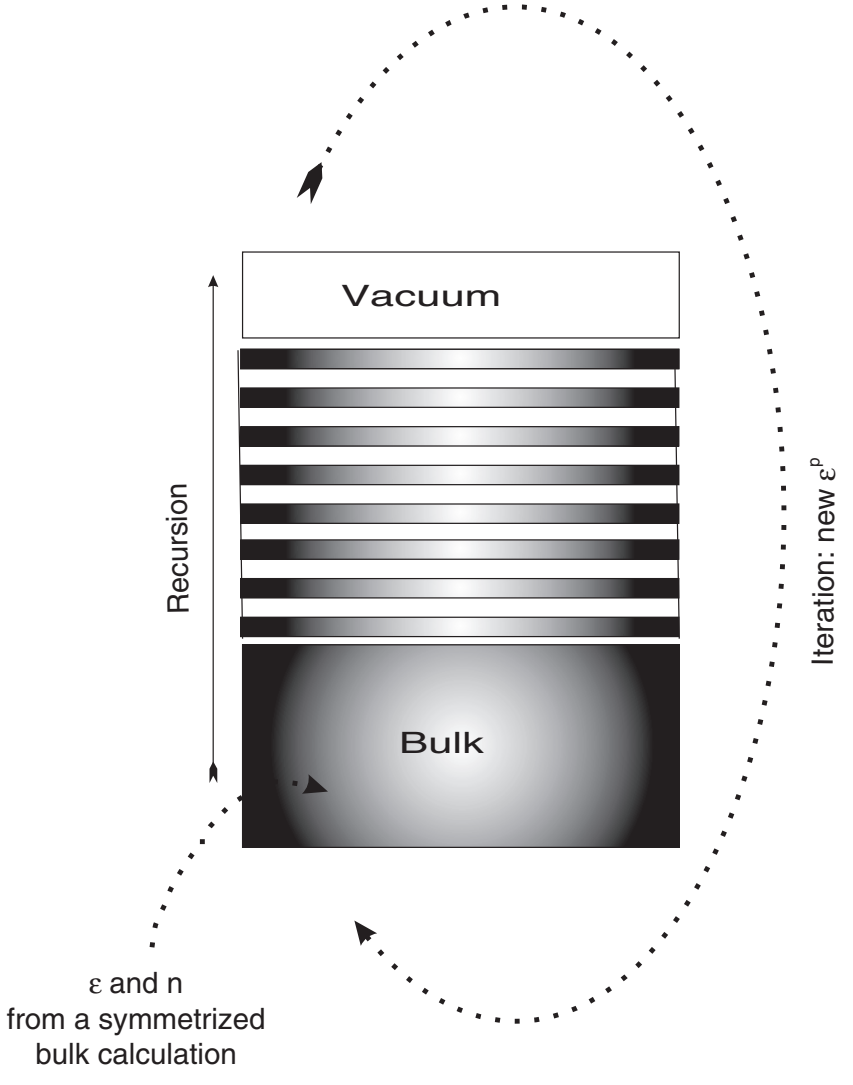

Figure 2. Recursive algorithm. Firstly, the bulk properties $\boldsymbol{\varepsilon}(\omega)$ and $\boldsymbol{n}(\omega)$ serving as the starting values for a layer recursion have to be known from a separate bulk calculation. Secondly, the 2×2 matrix technique starts at the boundary between the bulk and the first layer considered. Subsequently all reflections, transmissions and interferences at all boundaries between different layers are taken into account. Thirdly, the obtained layer-resolved permittivities $\boldsymbol{\varepsilon}^p(\omega)$ serve as input for the next iteration. This recursive approach is repeated until the desired accuracy for the permittivities $\boldsymbol{\varepsilon}^p(\omega)$ is obtained.

This system of equations for $\boldsymbol{\varepsilon}^p(\omega)$ (see equation (18)) has to be solved iteratively (figure 2), starting with

$$\overline{\mathbf{W}}_p^{(0)} = \mathbf{1}, \tag{25}$$

implying that

$$\boldsymbol{\varepsilon}^p(\omega)^{(0)} = \sum_{q=1}^{N} \boldsymbol{\varepsilon}^{pq}(\omega).$$

As a criterion for the accuracy of this iterative procedure the below inequality can be used

$$\left\| \boldsymbol{\varepsilon}^p(\omega)^{(n)} - \boldsymbol{\varepsilon}^p(\omega)^{(n+1)} \right\| < \boldsymbol{\varepsilon}^p(\omega)^{\text{threshold}}. \tag{26}$$

3.2. *Bulk systems*

As described above, the recursive algorithm starts at the interface between the substrate and first layer and ends at the interface between the last layer and the vacuum. In order to obtain the necessary bulk quantities $\mathbf{A}_0$ and $\mathbf{N}_0$ as starting values, the bulk properties $\boldsymbol{\varepsilon}_{\text{bulk}}$ and $\boldsymbol{n}_{\text{bulk}}$, have to be investigated. By definition in a bulk system ('infinite system', with three-dimensional periodicity) all physical properties have to be the same in all unit cells. For a simple lattice (one atom per unit cell) this implies that all physical quantities have to be the same in all (atomic) layers. As in the above algorithm the total number (N) of atomic layers necessarily has to be finite, in the case of a bulk system a kind of symmetric extension of the layered system such that $|p-q| \leqslant N-1$ with respect to a particular p can be applied by which the corresponding ε_{ij}^p, $i, j \in \{x, y, z\}$, are obtained as

$$\begin{aligned} \boldsymbol{\varepsilon}^p = & \sum_{q=p-N+1}^{0} \mathbf{W}^{N,N-|p-q|} \boldsymbol{\varepsilon}^{N,N-|p-q|} \\ & + \sum_{q=1}^{N} \mathbf{W}^{p,q}\ \boldsymbol{\varepsilon}^{p,q} + \sum_{q=N}^{p+N-1} \mathbf{W}^{1,1+|p-q|}\ \boldsymbol{\varepsilon}^{1,1+|p-q|}, \end{aligned} \tag{27}$$

namely as the original sum plus the extensions to the left and to the right.

§4. Results

Figure 3 shows schematically the types of calculation that have to be carried out. As a first step the effective scattering potentials for bulk Au and a free surface of Au along the (100) surface normal were calculated using the fully relativistic screened Korringa–Kohn–Rostoker method (Szunyogh *et al.* 1994, 1995, Újfalussy *et al.* 1995) and the local density functional parametrization by Vosko *et al.* (1980).

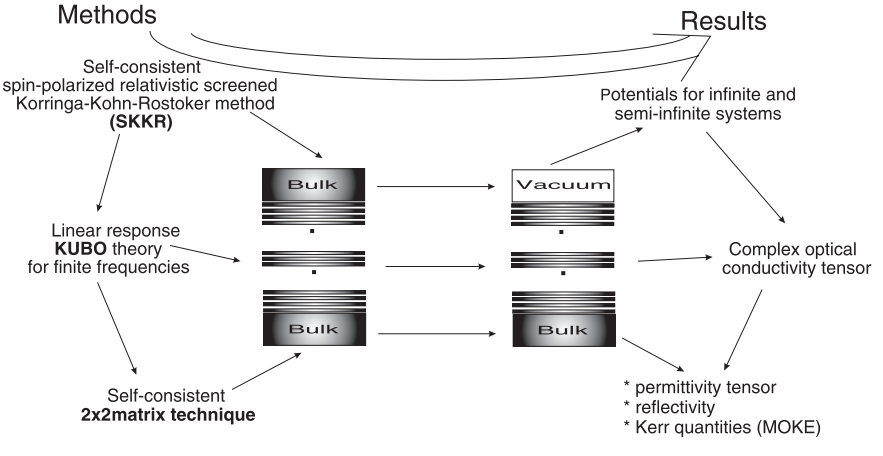

Figure 3. Computational scheme for an *ab initio* calculation of optical properties.

Next, the (complex layer-resolved) conductivity matrices $\boldsymbol{\sigma}_{\mu\nu}(\omega)$ are evaluated using the Kubo–Greenwood equation fully relativistically (Vernes *et al.* 2002c). Only then, as a third step, can the above-described calculation of the optical properties of Au be performed. In using this scheme the permittivities $\boldsymbol{\varepsilon}(\omega)$ for bulk Au and a free surface of Au along (100) were calculated for photon energies $\hbar\omega$ varying from 1.5 to 4 eV.

Let $\Delta_\varepsilon(N)$ be the difference between the in-plane and out-of-plane components of the permittivity:

$$\Delta_\varepsilon(N) = |\varepsilon_{xx}(N) - \varepsilon_{zz}(N)|,$$

where N is the total number of layers considered. Since in a bulk cubic system characterized by three-dimensional periodicity these two components have to be the same, that is

$$\lim_{N\to\infty} [\Delta_\varepsilon(N)] = 0,$$

$\Delta_\varepsilon(N)$ can serve as a numerical criterion for the calculated bulk permittivities. In figure 4, $\Delta_\varepsilon(N)$ is shown with respect to N together with the relative differences $2\Delta_\varepsilon(N)/|\varepsilon_{xx}(N) + \varepsilon_{zz}(N)|$, $\Delta_\varepsilon(N)/|\varepsilon_{xx}(N)|$ and $\Delta_\varepsilon(N)/|\varepsilon_{zz}(N)|$.

For bulk Au the present theoretical results compare reasonably well with the experimental data obtained by Hagemann *et al.* (1975) and Weaver *et al.* (1981). The principal shapes of the curves look alike; for small photon energies, $\boldsymbol{\varepsilon}(\omega)$ assumes quite large values (figure 5) owing to the finite lifetime broadening δ (see equation (1)).

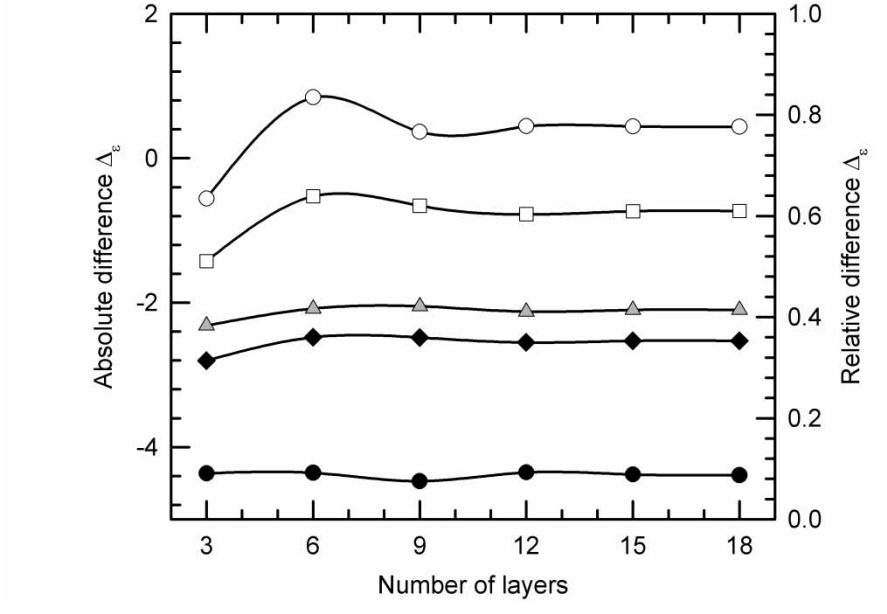

Figure 4. Convergence of the Au calculation to 'bulk' with respect to the number of Au layers sandwiched between two semi-infinite systems of Au, where the layer quantities are bulk like if the difference between the out-of-plane (ε_{zz}) and the in-plane components (ε_{xx} and ε_{yy}) of the permittivity vanishes: (●), Re (Δ_ε) (ordinate is the left y axis); (○), Im (Δ_ε) (ordinate is the left y axis); (◆), $|2\Delta_\varepsilon|/|\varepsilon_{xx} + \varepsilon_{zz}|$; (△), $|\Delta_\varepsilon|/|\varepsilon_{xx}|$; (□) $|\Delta_\varepsilon|/|\varepsilon_{zz}|$. For the relative differences the ordinate to the right applies.

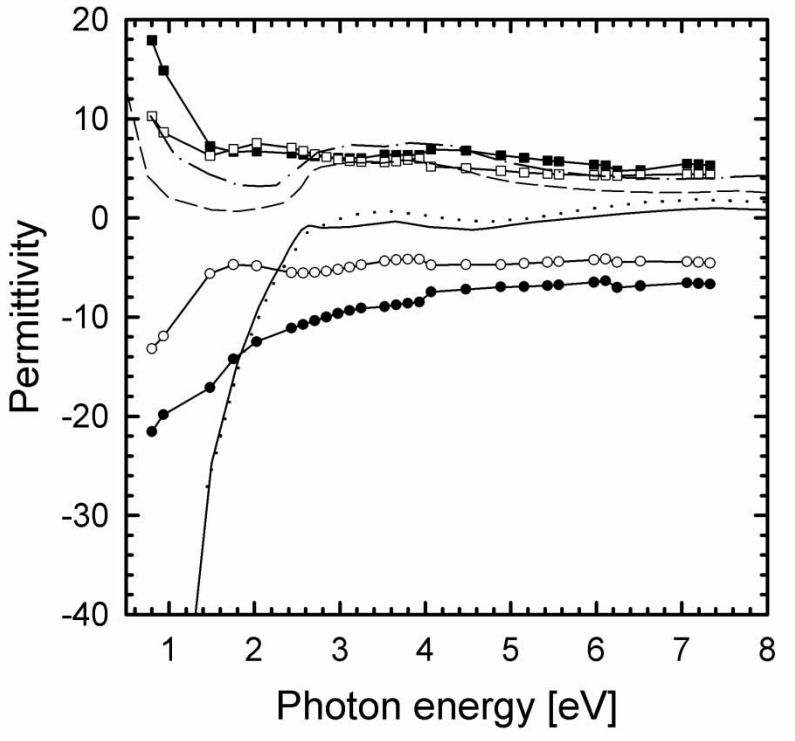

Figure 5. Permittivity for bulk Au: (——), experimental Re (ε_{xx}) values (Weaver *et al*. 1981); (- - - -) experimental values Im (ε_{xx}) (Weaver *et al*. 1981); (· · · · ·), experimental Re (ε_{xx}) values (Hagemann *et al*. 1975); (— · —), experimental Im (ε_{xx}) values (Hagemann *et al*. 1975); (●), theoretical Re (ε_{xx}) values; (■), theoretical Im (ε_{xx}) values; (○), theoretical Re (ε_{zz}) values; (□), theoretical Im (ε_{zz}) values.

Using now the results of the bulk calculation as initial values in equations (14) and (15), $\boldsymbol{\varepsilon}(\omega)$ was investigated for an Au(100) surface. It turns out that the order of magnitude of the theoretical permittivity differs considerably from the experimental data obtained by Bader *et al*. (2000) and by Truong *et al*. (2003), which in turn differ considerably from each other. In order to take into account these differences in figures 6–9, showing the real and imaginary parts of ε_{xx} and ε_{zz}, the experimental data are shifted and therefore different ordinates apply.

It should be mentioned that Au surfaces usually suffer somewhat from surface reconstruction. In the experiments of Bader *et al*. (2000) the surface was produced by depositing Au nanoparticles in a solvent on to a glass plate and evaporating the solvent afterwards. In the experiments of Truong *et al*. (2003), Au was evaporated onto glass substrates and annealed for 2 h. Thus, depending on the method of preparation, fundamental differences in the surface structure of Au can exist. Quite clearly the present calculations refer to a perfect single-crystal surface. Besides the fact that the experimental ambiguities affect the absolute size of the permittivity, all surface investigations (both experimental work (Bader *et al*. 2000, Truong *et al*. 2003) and the present theoretical study) detect one common feature, namely an anomalous adsorption at the surface, an effect which is not present for bulk Au. It is indeed reassuring that in all three studies the photon energies at which the peak in the permittivity occurs have rather similar values.

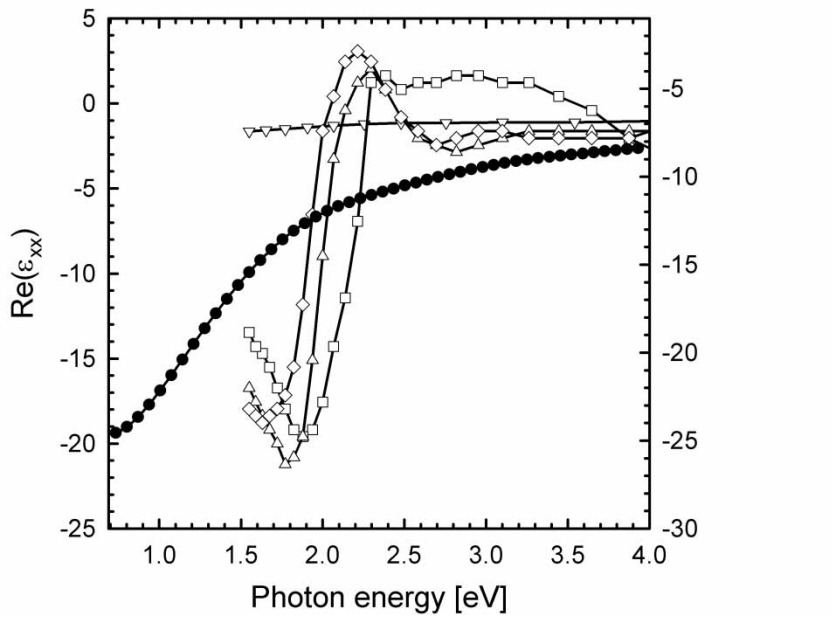

Figure 6. Re(ε_{xx}) for Au(100): (●), calculated values; (□), (△), (◇), experimental data for the 3 nm, 7.5 nm and 10 nm Au films respectively used by Truong *et al.* (2003); (▽), experimental data of Bader *et al.* (2000). The left ordinate applies to the experimental data, and the right to the calculated values.

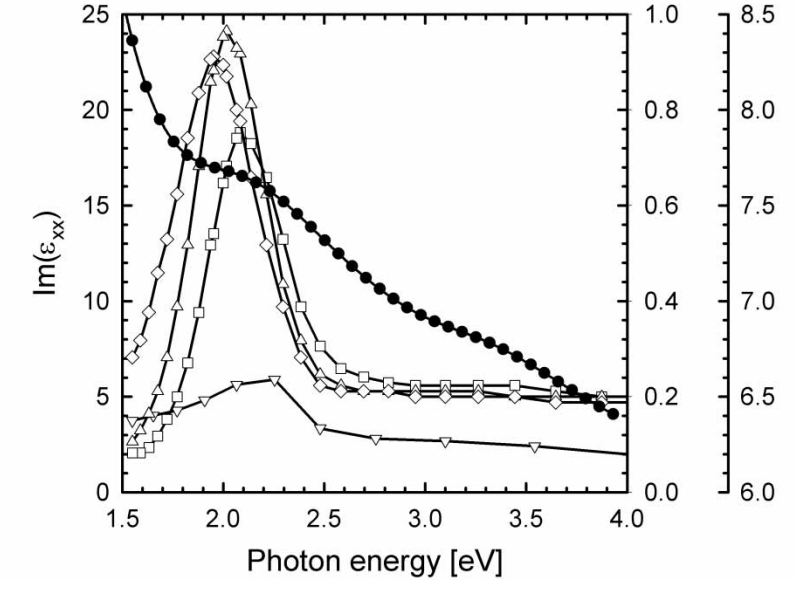

Figure 7. Im (ε_{xx}) for Au(100): (●), calculated values; (□), (△), (◇), experimental data for the 3 nm, 7.5 nm and 10 nm Au films respectively used by Truong *et al.* (2003), (▽), experimental data of Bader *et al.* (2000). The outer right ordinate applies to the calculated values, the inner right ordinate to the experimental data of Bader *et al.* (2000), and the left to all other values.

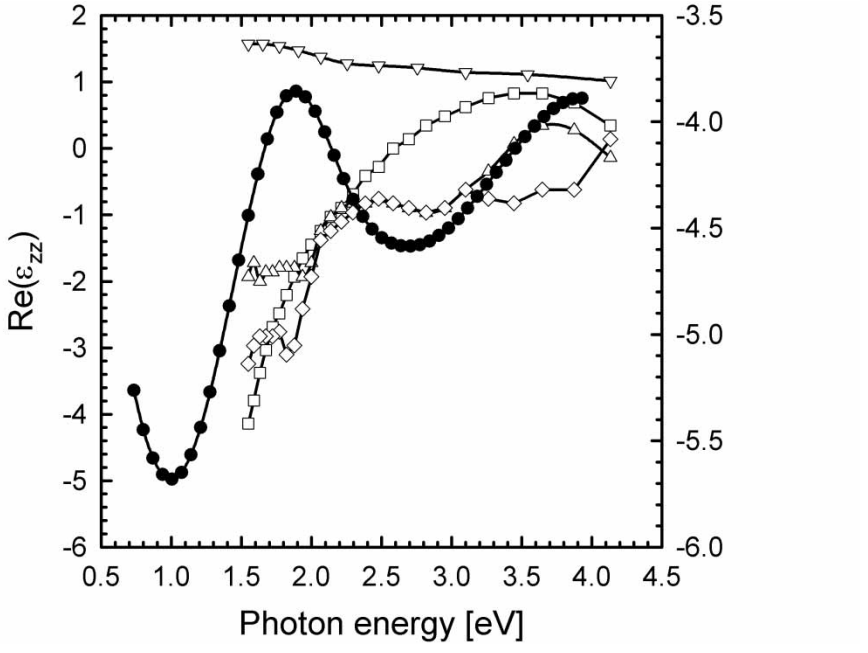

Figure 8. Re(ε_{zz}) for Au(100): (●), calculated values; (□), (△), (◇), experimental data for the 3 nm, 7.5 nm and 10 nm Au films respectively used by Truong *et al*. (2003); (▽), experimental data of Bader *et al*. (2000). The left ordinate applies to the experimental data, and the right to the calculated values.

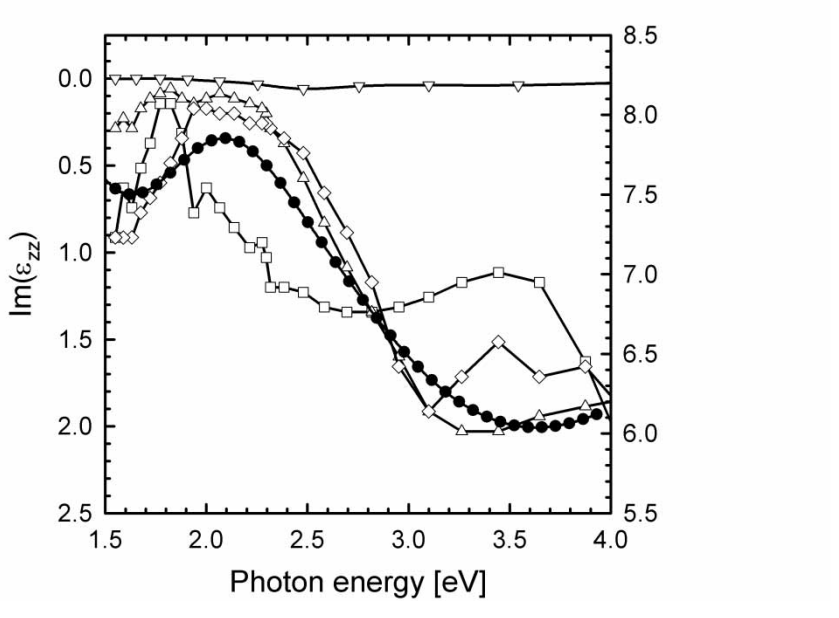

Figure 9. Im (ε_{zz}) for Au(100): (●), calculated values; (□), (△), (◇), experimental data for the 3 nm, 7.5 nm and 10 nm Au films respectively used by Truong *et al*. (2003); (▽), experimental data of Bader *et al*. (2000). The right ordinate applies to the calculated values, and the left to the experimental data.

It should be noted that, independent of the film thickness, always only two-dimensional rotational symmetry applies. Therefore all investigations of the permittivity show different results for the ε_{xx} and the ε_{zz} components. The calculated values of $\mathrm{Re}\,(\varepsilon_{xx})$ for Au(100), (see figure 6) have a maximum at about 1.9 eV, and a kind of ondulation at approximately 2.4 eV, which also can be seen in the experimental values at 2.4 eV for the thinnest film and at 2.2 eV for the thickest film. The calculated values of $\mathrm{Re}\,(\varepsilon_{zz})$ for Au(100), appear to be in reasonably good qualitative agreement with the measured data (Truong *et al.* 2003), although $\varepsilon_{zz}(\omega)$ seems to depend strongly on the film thickness. For instance, the experimental curves for 3 nm and 7.5 nm film thicknesses change sign at photon energies above 2.6 eV and 3.4 eV respectively while the calculated curve and the curve measured for 10 nm do not change sign below 3.5 eV.

§ 5. Conclusion

It was shown in this paper that, by mapping the quantum-mechanically evaluated conductivity tensor on to the macroscopic permittivity tensor and by applying an appropriate scheme for taking into account all interferences and reflections, optical properties can be studied on a truly *ab initio* level. The present study also showed that, whenever realistic systems, that is systems with a surface, have to be dealt with, a comparison with experimental data has to be carried out with extreme care since, not only can the applied preparation technique be decisive, but also the thickness of the prepared films enters the experimental observations. It also has to be noted that the term 'bulk' in many cases can be quite misleading, not only because any kind of measurement is carried out 'from the outside', that is for an at best semi-infinite system, but also because 'bulk' very often only refers to a fictitious quantity, obtained by extrapolating certain thickness parameters to infinity. In the present study the permittivity of 'bulk' Au is needed as starting value for an a iterative procedure aiming at an evaluation of the surface reflectivity. Keeping in mind that, as mentioned in the introduction, optical measurements are of crucial importance for the characterization of magnetic properties of multilayered systems, heterostructures, etc., in terms of the Kerr effect a rigorous study of the optical properties of a typical substrate is very necessary.

Acknowledgements

Financial support from the Austrian Science Foundation (project W004), the Austrian Science Ministry (GZ 45.531) and the Wissenschaftlich-Technisches Abkommen (WTA) Austria–Hungary (A-3/03) is gratefully acknowledged. We also wish to thank the computing centre IDRIS at Orsay as part of the calculations was performed using their facilities.

References

Bader, G., Haché, A., and Truong, V.-V., 2000, *Thin Solid Films*, **375**, 73.
Hagemann, H. J., Gudat, W., and Kunz, C., 1975, *J. opt. Soc. Am.*, **65**, 742.
Mansuripur, M., 2002, *Classical Optics and its Applications* (Cambridge University Press).
Szunyogh, L., Újfalussy, B., Weinberger, P., and Kollar, J., 1994, *Phys. Rev.* B, **49**, 2721.
Szunyogh, L., Újfalussy, B., and Weinberger, P., 1995, *Phys. Rev.* B, **51**, 9552.
Szunyogh, L., and Weinberger, P., 1999, *J. Phys. condens. Matter*, **11**, 10 451.
Truong, V.-V., Belley, R., Bader, G., and Haché, A., 2003, *Appl. Surf. Sci.*, **212**–**213**, 140.

VERNES, A., SZUNYOGH, L., and WEINBERGER, P., 2002a, *Phys. Rev.* B, **65**, 144 448; 2002b, *ibid.*, **66**, 214 404; 2002c, *Phase Transitions*, **75**, 167.

VOSKO, S. H., WILK, L., and NUSAIR, M., 1980, *Can. J. Phys.*, **58**, 1200.

ÚJFALUSSY, B., SZUNYOGH, L., and WEINBERGER, P., 1995, *Phys. Rev.* B, **51**, 12 836.

WEAVER, J. H., KRAFKA, C., LYNCH, D. W., and KOCH, E. E., 1981, *Optical Properties of Metals* (Fach-Informationszentrum Karlsruhe).

WELLER, D., 1995, *Spin–orbit-influenced Spectroscopies of Magnetic Solids*, edited by H. Ebert and G. Schütz (Berlin: Springer), p. 1.